A Quantum Statistical Model of Decision Making in a Single-Cell Eukaryote

Jad Soucar (soucar@usc.edu)
USC Viterbi Daniel J. Epstein Department of Industrial & Systems Engineering 3715 McClintock Avenue
Los Angeles, CA 90089-0193 USA

Francis F. Steen (steen@comm.ucla.edu)
Department of Communication, 345 Portola Plaza,
Los Angeles, CA 90095, USA

Abstract

The single-celled protist Stentor roselii has long been observed to exhibit complex decision-making behaviors, yet existing machine learning and classical computational models have struggled to replicate its actions. In this paper, we propose a novel quantum-statistical framework to model S. roselii's behavioral responses to environmental stimuli. By leveraging quantum circuits with amplitude dampening and memory effects, we construct a quantum behavioral model that captures the probabilistic and hierarchical nature of S. roselii's decision-making. Our results suggest that quantum statistical theory provides a promising tool for representing and simulating biological decision processes.

Keywords: Decision making, Unicellular cognition, Stentor roselii, Quantum computing, Quantum statistics, Biological computation

Introduction

Complex behavior that requires collecting information from the environment and formulating an appropriate conditional response has generally been thought to require specialized cells – networks of neurons – dedicated to this task. However, recent work has shown that single neurons are capable of surprisingly complex computations (Quian Quiroga et al., 2023) and that even single-celled organisms have the capacity to display conditional behaviors. These findings offer a potential opening for new models for understanding low-level biological decision-making and cognition. Here, we examine certain aspects of the behavior of Stentor roselii, a unicellular eukaryote.

In 1906, the biologist Herbert Spencer Jennings reported that Stentor roselii exhibited signs of complex behavior, potentially indicating a form of decision-making (Jennings, 1931). Jennings' work seemed to indicate that the protist was capable of choosing from a set of possible actions and that the choice was dependent on past experiences. Long thought to be discredited as unreplicable, a team led by Gunawardena (Dexter, Prabakaran, & Gunawardena, 2019) recently successfully replicated and expanded on Jennings' findings, quantifying the behavior of Stentor roselii within a dataset that is now publicly available, and concluding that the protist was exhibiting a form of structured decision making.

Using Jenning's and Dexter's findings, researchers have sought to develop learning models capable of reproducing the protists' behavior. For example, in 2016 Staddon graded the documented set of Stentor roselii's avoidance behaviors according to the energy required and the opportunity cost associated with carrying out each strategy using qualitative behavioral theories (Staddon, 2016). Others have applied quantitative machine learning models such as decision trees, random forests, and artificial feed-forward neural networks. However, these models fall short of fully capturing the behavior demonstrated in Dexter's experiments, with the best modeling producing an accuracy of roughly 59% (Trinh, Wayland, & Prabakaran, 2019). Trinh et al. conclude that Stentor roselii's decision-making process "cannot be fully explained by habituation, sensitization or operant behavior" (Trinh et al., 2019).

In order to develop an accurate and biologically plausible model, as well as introduce a new tool to the body of literature on this problem, we first motivate and then propose a novel quantum statistical framework for modeling the protist's documented avoidance behavior. Our aim is to computationally replicate Dexter's statistical findings while also providing a framework capable of capturing more complex representations of the protist's behavioral biases and cognitive schema. To do this, we first analyze Stentor roselii's behavior, next we motivate the application of quantum statistical theory, before finally proposing and testing a quantum behavioral model of Stentor roselii.

Behavior of Stentor Roselii

Jennings reported a hierarchy of avoidance behaviors that the protist exhibited when exposed to an irritant or toxin (Jennings, 1931; Dexter et al., 2019). We list the behaviors in the same sequence Jennings reported they occurred; resting (R), bending away (B), ciliary alteration (A), contraction (C), and detachment from the surface (D). Gunawardena's team concluded that there is strong statistical evidence that Stentor roselii follows the ordered $(R-B-A-C-D)$ behavioral hierarchy. However, they note that the hierarchy was rarely observed in full and that they instead observed many partial instances of the hierarchy with cases of the protist skipping steps. The one exception to the skipping phenomenon is that detachment (D) is always the last behavior exhibited. According to (Staddon, 2016), (A/B) are low-energy actions, while (C) and (D) require more energy to execute. This suggests that the observed hierarchy accords with optimal foraging theory, which posits that organisms evolve to minimize energy expenditure while maximizing energy intake (Pyke, 2019). In the following section we investigate whether the step-skipping is structured in a manner consistent with optimal foraging theory.

In D. Barner, N.R. Bramley, A. Ruggeri and C.M. Walker (Eds.), *Proceedings of the 47th Annual Conference of the Cognitive Science Society*

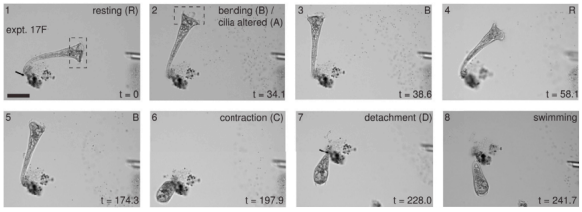

Figure 1: An observed sequence of behaviors (Dexter et al., 2019)

Statistical Analysis

Dexter's dataset is formatted as a set of sequences formed by A,B,C,D with interspersed pluses (p) indicating instances where the researchers manually injected a toxin into the protist's environment. For example, a sequence may look like "ABpACCpCCCD" or "CpCCD". Given the structure of the data, we define inter-sequence and intra-sequence trends. Inter-sequence trends deal with the protist's decision making up until the toxin is eliminated and then reintroduced using a pulse. Intra-sequence trends deal with how decision-making changes across multiple interactions.

First we cover the inter-sequence trends. It is simple to observe in Dexter's data that (A/B) never follows (C) except for two samples, which Dexter attributes to accidental pulses. In other words, once a series of contractions begins, the protist will return to a resting state only after a detachment or a behavior that successfully evades the toxin. Dexter observed that when the protist contracts (C) there is a 50% chance the contraction will be followed by a detachment (D), and that the probability of remaining attached after k consecutive contractions is $\frac{1}{2^k}$. This indicates that the decision to detach (D) post contraction was tantamount to a coin flip. Through an analysis of Dexter's dataset, we note that the (A/B) action had a success rate of approximately 10%, (C) was successful around 50% of the time and (D) had a 100% success rate. These results indicate that the cheaper (A/B) actions were less effective in eliminating the toxin from the protist's environment and that the contraction was evaluated to be successful at the rate of a fair coin flip.

Regarding intra-sequence trends, Dexter's experiments indicated that (A) and (B) often occurred together and consequently can be treated as a single action (A or/and B). Using this notational adjustment, we note that the first action taken by a protist with no immediate history of interacting with toxins is (A/B). Additionally, Dexter notes that all 44 instances of (D) were directly preceded by (C) and that in 30/44 instances, (D) was preceded by (A or/and B). This means that in roughly 30% of cases, the (A/B) action was skipped entirely. We note that this corresponds with the 30% conditional probability that (A/B) is reapplied, given that (A/B) failed to remove the toxin in the protist's most recent interaction. This is consistent with the hypothesis that the protist learned that the (A or/and B) response was frequently not sufficient to eliminate the toxin and consequently opted for the more energy-intensive option of contracting (C) immediately after the second encounter with the toxin (Marshall, 2019).

We conclude by noting that an analysis of Dexter's data indicates that a single-celled organism can perform a range of computational tasks conducive to survival, ranging from detecting and responding to environmental stimuli to learning statistically optimal behavior.

Motivation for a Quantum Model

Based on their statistical analyses, both Dexter and Jennings conclude that Stentor roselii possesses the capacity for hierarchical decision making. A growing body of work acknowledges that relatively complex information processing is taking place inside cells (Gershman, Balbi, Gallistel, & Gunawardena, 2021; Picard & Shirihai, 2022a; Fitch, 2023). Since information processing is necessarily metabolically costly (Laughlin, de Ruyter van Steveninck, & Anderson, 1998; Fields & Levin, 2021), intracellular information processing creates persistent adaptive pressures to avoid heat waste and to miniaturize – adaptive targets that may favor quantum processes. Both experiments and simulations confirm that living systems have recruited quantum processes to optimize energy capture in light harvesting (Fleming, Scholes, & Cheng, 2011; B.-X. Wang et al., 2018; Uthailiang, Suntijitrungruang, Issarakul, Pongkitiwanichakul, & Boonchui, 2025).

Bray proposes that intracellular information processing is realized by biochemical pathways that act like classical logic circuits or neural networks, conceding that the key difference between electronic and biological circuits is that cellular circuitry is noisy and its outcomes can be difficult to predict (Bray, 2009). Precisely these features open for the possibility that biological systems diverge from classical logic circuits and recruit the noisy and probabilistic characteristics of quantum circuits. In the following, we explore the possibility that the behavior of Stentor roselii is best described not by neural networks or other deterministic and digital imitations of biological wetware, but instead through quantum circuits. While our target is a single-celled organism, we recognize a potentially fruitful overlap with the quantum statistical approach to cognition (Pothos & Busemeyer, 2013; Z. Wang, Busemeyer, Atmanspacher, & Pothos, 2013; Yukalov & Sornette, 2014).

Proposed Quantum Behavioral Model

In this section we describe a iterative quantum circuit that statistically captures the Stentor roselii's behavior. First we introduce a 2 qubit state vector $|\psi\rangle$ where the measurement outcome $|11\rangle$ is the the (A/B) action, $|10\rangle$ is contraction (C), $|01\rangle$ is detachment (D), $|00\rangle$ is the resting state. We can represent $|\psi\rangle$ as the tensor product of two qubit $|\psi_1\rangle \otimes |\psi_2\rangle$ or as 4×1 vector where r, c, ab, d correspond with the square root of the probability that the protist will choose to rest (R), contract (C), deploy the (A/B) action, or detach (D) respectively.

$$|\psi\rangle = \begin{pmatrix} r \\ d \\ c \\ ab \end{pmatrix} = |\psi_1\rangle \otimes |\psi_2\rangle \tag{1}$$

Secondly, we introduce a toxin qubit $|p\rangle$ which is $|1\rangle$ when a toxin is present and $|0\rangle$ when there is no toxin detected. We note that $|p\rangle$ is functionally a digital bit in that it will only ever take on 0 or 1 value. We also introduce a memory qubit $|m\rangle$ which allows the protist to store its previous action. Specifically if $|m\rangle = |0\rangle$ the previous action was (A/B), if $|m\rangle = |1\rangle$ the previous action was (C), if $|m\rangle = |-\rangle$ then the previous action was (D), and if there was no previous action then $|m\rangle = |+\rangle$. So the full state of the protist, which contains the internal state qubits and environmental data qubits, can be written as $|\psi\rangle \otimes |m\rangle \otimes |p\rangle$. For example, assuming the $|p\rangle$ is initially set to $|0\rangle$ (no toxin), we can describe a protist who has entered a toxic environment using the following circuit.

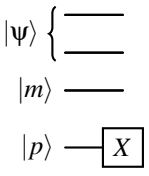

where X is the Pauli X gate, which flips the qubit its applied to and in this case "turns on" the toxin bit.(Nielsen & Chuang, 2012). Next we describe the mechanism through which the protist adjusts the probability of an action based on the state of $|p\rangle$. In quantum circuits the process of increasing or decreasing the probabilities of certain outcomes can be replicated through amplitude dampening, a rotation based mechanism which decreases the probability of a certain outcome using quantum gates. We will use amplitude dampening to adjust the inter-sequence and intra-sequence statistics of the protist. For example, given that the $|\psi\rangle = \big(0,0,0,1\big)$, which would indicate that the protist will definitively choose (A/B) as its next action, one could decrease the probability of choosing (A/B) after a failed application using a Givens Rotation $G_{AB,C}(\theta)$. θ would represent the inter-sequence learning rate, or how quickly the protist changes its preference between (A/B) and (C).

$$G_{AB,C}(\theta) = \begin{pmatrix} 1 & 0 & 0 & 0 \\ 0 & 1 & 0 & 0 \\ 0 & 0 & \cos\theta & \sin\theta \\ 0 & 0 & -\sin\theta & \cos\theta \end{pmatrix} \tag{2}$$

We also define a controlled G gate which outlines the various adjustments a protist can make. First, if the previous action was an unsuccessful (A/B), then the protist decreases the probability of choosing (A/B) again and increases the probability of choosing (C). On the other hand, if the last action was an unsuccessful (C), then the protist maps $|\psi\rangle$ to $|t\rangle = \frac{1}{\sqrt{2}}\begin{pmatrix} 0 & 1 & 1 & 0 \end{pmatrix}$ for two reasons. First, after the protist chooses a contraction, the probability of returning to (A/B) before the end of the sequence drops to 0. Second, it represents the 50/50 chance, which Dexter observed, that (C) is reapplied or the protist detaches (D). Lastly if an action was successful and the toxin bit $|p\rangle = |0\rangle$, then the protist returns to a resting state $|\psi\rangle = |00\rangle$. This process can be model using G, where $U_{|\phi\rangle}(|\psi\rangle) : |\psi\rangle \mapsto |\phi\rangle$.

$$G(|m\rangle, |p\rangle) = \begin{cases} G_{AB,C}(\theta), & \text{if } |m\rangle = |0\rangle \text{ and } |p\rangle = |1\rangle \\ U_{|t\rangle}(|\psi\rangle), & \text{if } |m\rangle = |1\rangle \text{ and } |p\rangle = |1\rangle \\ U_{|00\rangle}(|\psi\rangle), & \text{if } |p\rangle = |0\rangle \end{cases} \tag{3}$$

Using these tools we can begin to piece together a quantum circuit that reflects the behavior of Stentor roselii. We begin by setting the initial state of the system to $|00+0\rangle$, which represents a resting state with no toxins detected and no recorded last action. In order to simulate the presence of a toxin we apply $X \otimes X \otimes I \otimes X$ which flips the toxin bit, guarantees a first response of (A/B), and yields the following state $|11+1\rangle$. We set the probability of (A/B) to 1, since this is the default starting action for a protist as observed in Dexter's experimental data. Next we measure the first two qubits of the circuit $|\psi\rangle$ and find that the $|\psi\rangle$ has collapsed to $|11\rangle$ and the protist has chosen (A/B). Based on that response, we record the last action in $|m\rangle$ using the following gate:

$$M = \begin{cases} U_{|+\rangle}(|m\rangle), & \text{if } |\psi\rangle = |00\rangle \\ U_{|0\rangle}(|m\rangle), & \text{if } |\psi\rangle = |11\rangle \\ U_{|1\rangle}(|m\rangle), & \text{if } |\psi\rangle = |10\rangle \\ U_{|-\rangle}(|m\rangle), & \text{if } |\psi\rangle = |01\rangle \end{cases} \tag{4}$$

In this case the measurement outcome is $|11\rangle$, which corresponds to the (A/B) action and will trigger a bit-flip noise operation $X_{\hat{p}}$ applied to $|p\rangle$ at a probability $\hat{p}$ (Nielsen & Chuang, 2012), where $\hat{p}$ is 0.10 as observed in Dexter's dataset. However in general $X_{\hat{p}}$ can be determined by the following function. Notice that the probability of flipping the toxin bit to $|0\rangle$ is 0 when the protist is at rest and 1 when the protist has detached.

$$X_{\hat{p}} = \begin{cases} X_0, & \text{if } |m\rangle = |+\rangle \\ X_{\frac{1}{10}}, & \text{if } |m\rangle = |0\rangle \\ X_{\frac{1}{2}}, & \text{if } |m\rangle = |1\rangle \\ X_1, & \text{if } |m\rangle = |-\rangle \end{cases} \tag{5}$$

Next we measure the toxin qubit $|p\rangle$ to determine whether or not the action was successful. If the action was successful and $|p\rangle = |0\rangle$, we apply $G_1 \leftarrow U_{|00\rangle}(|\psi\rangle)$, which returns the protist to a resting state. This process can be represented using the following quantum circuit. It is important to note that we assume the measurement on $|\psi\rangle$ does not de-cohere the state. While this is simple to do within a classical simulation, implementing a coherent measurement within a quantum computer is more involved and is discussed in the following section.

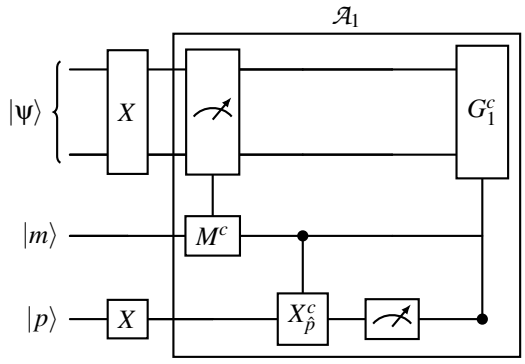

Now assume that we measure $|p\rangle = |1\rangle$, then we conclude that the previous action was unsuccessful in eliminating the toxin. The protist measures $|m\rangle$ and determines that the last action was (A/B), which prompts it to decrease the probability of choosing (A/B) using $G_1 \leftarrow G_{AB,C}(\theta)$ with some inter-sequence learning rate θ. The state is then measured again to determine the next action. This process continues until the toxin is removed, which requires the measurement of $|p\rangle$ to return $|0\rangle$, or the measurement of $|\psi\rangle$ to return $|10\rangle$, which corresponds with the (C) action. Assuming we measure $|\psi\rangle$ to be $|10\rangle$ (C) on the n^{th} iteration then $X_{\hat{p}} \leftarrow X_{\frac{1}{2}}$. If the toxin remains, we apply $G_n \leftarrow U_{|t\rangle}(|\psi\rangle)$, which sets the probability of choosing (C) to the statistically predicted rate of $\frac{1}{2}$. We repeat this process and continue to apply $U_{|t\rangle}(|\psi\rangle)$, which decreases the probability of (C) to $\frac{1}{\sqrt{2}^k}$ after k failed (C) applications, until a measurement on $|\psi\rangle$ yields the detachment state (D) $|01\rangle$. At this point $X_{\hat{p}} \leftarrow X_1$, which flips $|p\rangle$. In other words, the toxin is eliminated and the sequence terminates.

While the sequence itself has terminated, the protist will still use the sequence to inform future decisions. Recall the statistical analysis which showed that in 70% of cases where (D) was not preceded by (A or/and B) the protist had already tried and failed to apply the (A or/and B) response to an earlier interaction with the toxin. This indicated that upon a failed application of (A/B), the probability that the protist chooses (A/B) as a first response in the next interaction with a toxin decreases to 30% while the probability of (C) increases to 70%. Therefore, once the protist terminates the sequence and begins an interaction with another toxin, we allow the protist to access its memory and adjust its bias towards one decision or another. In practice, this is accomplished by applying the following function R, where $|c\rangle = \begin{pmatrix}0 & 0 & \sqrt{0.7} & \sqrt{.3}\end{pmatrix}$ and $|ab\rangle = \begin{pmatrix}0 & 0 & \sqrt{0.3} & \sqrt{.7}\end{pmatrix}$ once the sequence terminates. Notice that if there is no previous actions, the protist defaults to the AB action.

$$R(|m\rangle) = \begin{cases} U_{|c\rangle}|\psi\rangle, & \text{if } |m\rangle = |1/-\rangle \\ U_{|ab\rangle}|\psi\rangle, & \text{if } |m\rangle = |0\rangle \\ X \otimes X, & \text{if} |m\rangle = |+\rangle \end{cases} \quad (6)$$

For example, assume that $|p\rangle$ is measured to be $|0\rangle$ on the n^{th} iteration. In that case, $G_n \leftarrow U_{|00\rangle}(|\psi\rangle)$, which sends the protist to a resting state. Once the toxin is detected again, which would entail manually applying an X gate to $|p\rangle$, the protist adjusts its decision bias by applying R to $|\psi\rangle$ before proceeding with the rest of the sequence. Notice that a full sequence, from the detection of a toxin to termination, can now be described compactly as the following circuit where $\{k_i\}$ is the set of iterations at which a sequence terminates. We note that an application of $\mathcal{B}$ is a user-level decision which is similar to Dexter's experimental setup where the researchers deliver toxins into an environment manually through the introduction of microbeads (Dexter et al., 2019). We also note that once the first sequence is over, we can apply $\mathcal{B}_2$ and $\{\mathcal{A}_i\}_{i=k_1+1}^{k_2}$, and so forth.

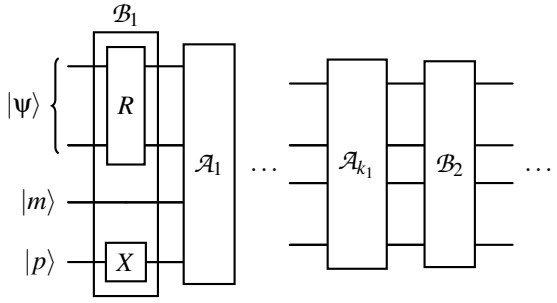

The Measurement Problem We note that measuring the $|\psi\rangle$ and $|p\rangle$ qubits is a commonly used tool in the quantum circuit described above. However, unlike traditional measurements, which collapse the qubits to a certain state, the measurement we apply is only meant to retrieve the probabilities associated with an action or the presence of a toxin. In fact the algorithm described above only operates as intended if the measurement does not decohere the state, since decohering $|\psi\rangle$ would correspond to the protist losing its internal representation of its action biases. This feature of the algorithm contradicts the standard Copenhagen interpretation of quantum mechanics, which does not allow for measurement without collapsing the quantum state (Wigner, 1963). We remain open to the possibility that biological processes may recruit quantum physics for information gathering without triggering decoherence, as has been claimed for the FMO complex, a light-harvesting protein found in green sulfur bacteria, where "reversible sampling" may play a critical role in directing excitation energy from antenna complexes to reaction centers (Fleming et al., 2011). Pilot Wave theory, an alternative interpretation of quantum physics that rejects the idea of a wave-function collapse and more generally of a "cut" between the quantum and classical realm, may provide a fruitful starting point for quantum biology (De Broglie, 1927), (Bohm & Bub, 1966), (Bohm & Hiley, 2006).

A possible work-around the measurement problem can be built using the use of "counter" qubits to count how many times the (AB) action has been successively applied to $|\psi\rangle$. This is done by storing "counter" qubits $|\phi_n\rangle = |\phi_1 \ldots \phi_n\rangle$ and applying an increment unitary circuit containing the Toffoli, CNOT, and X operation every time the (AB) action is chosen, where 2^n is the largest number of repetitions the counter can store. Once any action other then (AB) is chosen we return

$|\phi_1 \dots \phi_n\rangle$ to the $\left|\vec{0}\right\rangle$ through the use of state preparation gates, indicating that the counter is restarting (Nielsen & Chuang, 2012). Applying the following circuit repeatedly will iterate our counter from $|000\rangle \to |001\rangle \to \cdots \to |111\rangle$.

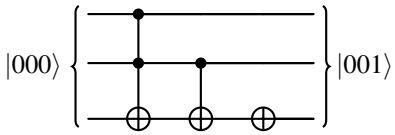

We are only concerned with the (AB) action because an action of (C) or (D) forces $|\psi\rangle$ to the specific states $|t\rangle$ or $|00\rangle$ respectively. In other words, only an (AB) action can yield a non-static state. This is not surprising, considering that when the (C) action is chosen, only (C) or (D) can be chosen next at a probability of $\frac{1}{2}$. In this case, once $|\psi\rangle$ is measured and as a result collapses to one action, we apply $\tilde{G}(|m\rangle, |p\rangle, |\phi_n\rangle)$, which is controlled by the counter. Simply put, if $|\phi_n\rangle = \left|\vec{0}_n\right\rangle$ then $\tilde{G} = G$, otherwise we restore $|\psi\rangle$ to its pre-measurement state by setting $\tilde{G} = G^{\Sigma_{i=0}^{n} 2^i \phi_i}$. Below is the circuit for $\tilde{G}$ that is used to execute this strategy. Note that if we wish to increase the counter's maximum we must add "counter" qubits, however in most cases the probability that AB is chosen more than 3 times is vanishingly small.

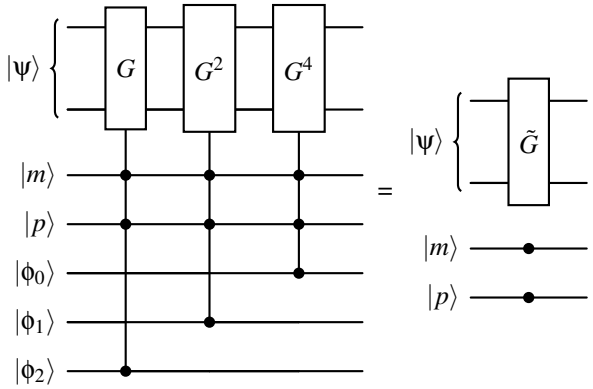

Estimating the Inter-Sequence Learning Rate θ

At this point an interesting question to ask is how quickly a protist learns that (AB) is an ineffective action strategy and pivots to contractions (C). To answer this, we first analyze the expected depth of each sequence given an initial state $|\psi_0\rangle$. First we let the random variable N be the number of iterations until termination. Second we note that the length of each sequence depends on the evolution of the probabilities of the (A/B) and (C) actions. So we let the state at the beginning of the sequence be $|\psi_0\rangle \in \mathbb{R}^2$, where ψ_1, ψ_2 are the probabilities of the (A/B) and (C) action respectively. We solve this problem for an arbitrary $|\psi_0\rangle$ and find $\mathbb{E}[N|\,|\psi_0\rangle]$. We note that this expectation can be broken up into an expectation of N_{AB}, which is the number of iterations before (C) is first chosen or an (A/B) action results in removal of the toxins, and N_C, which is the number of iterations before (D) is first chosen or (C) results in removal of the toxins.

$$\mathbb{E}[N|\,|\psi_0\rangle] = \mathbb{E}[N_{AB}|\,|\psi_0\rangle] + \mathbb{E}[N_C|\,|\psi_0\rangle] \tag{7}$$

We observe that $\mathbb{E}[N_C|\,|\psi_0\rangle] = 2$, since it is geometrically distributed with probability $1/2$, and we proceed to the calculation of $\mathbb{E}[N_{AB}|\,|\psi_0\rangle]$. For this computation, we introduce the $AB_n \in \{0,1\}$ random variable, where n is the number of iterations that (A/B) action was consecutively selected n times and a value of 0 represents an instance where (A/B) was not selected. We also note the following probability measure for (A/B), where ρ is the learning rate induced by $G_{A,B}(\theta)$:

$$\mathbb{P}(AB_n = 1) = \max(\psi_1 - \rho n, 0), \quad \mathbb{P}(AB \text{ Succeeds}) = .10 \tag{8}$$

Using these two measures, we conclude that the probability that the number of consecutive (A/B) actions is k is $\mathbb{P}(k) = \prod_{i=0}^{k} \frac{9}{10} * \max(\psi_1 - \rho n, 0)$.

$$\mathbb{E}[N_{AB}|\,|\psi_0\rangle] = \sum_{n=0}^{\infty} n\mathbb{P}(n) = \sum_{n=0}^{\lfloor \frac{\psi_0}{\rho} \rfloor} n(\psi_1 - \rho n). \tag{9}$$

Take $\rho = 0.1725$ and let $\psi_1 = 1$. We find that the $\mathbb{E}[N_{AB}|\,|\psi_0\rangle] = 2.44$, which is in line with the empirically determined expected depth of a sequence in Dexter's dataset (Dexter et al., 2019) [1]. This implies that $\theta = \cos^{-1}(1-\rho) = .59616$. We conclude by reiterating that the expected depth calculus can also serve as a powerful tool to calibrate the inter-sequence learning rate θ.

Quantum Advantage for High Complexity Models

We note that it may seem reasonable to apply Hidden Markov Models, Reinforcement Learning when our behavior model is of low-complexity. However once we add more complexity to the behavior model, such as p existing on a spectrum of $[0,1]$ and the organism retaining a larger memory bank, then a quantum model becomes a more natural choice that preserves model explainability. Namely by using a quantum model we can directly observe and quantify the degree to which current behavior is entangled with previous actions and how previous actions are entangled with each other (Nielsen & Chuang, 2012). In other words the quantum structure can shine light on how memory could be structured within a single celled organisms and how that memory effects current behavior. Additionally once more experimental data and corresponding environmental data becomes available we can apply work from Busemeyer et. al to investigate systematic biases associate with the protist's deicion making. For example the presence of certain environmental stimuli like acidity or food sources may lead to quantifiable interference patterns where certain stimuli reinforce or destroy certain behaviors (Z. Wang et al., 2013). Finally given recent research linking quantum effect to biological systems, a quantum model appears to be more biologically plausible and offers quantum theoretical support to future research linking biological mechanics of single celled organisms to quantum phenomenon.

[1] When calculating the empirical mean we, like Dexter, excluded as an outlier experiment 18B, in which the organism contracted 20 times after a single pulse.

Results

Now that we've conducted some model analysis and discussed the measurement problem, we will begin implementing our quantum model and analyzing the results. To do this end, we will perform the simulation using the model parameters computed earlier through our statistical analysis of Dexter's data; $\{|c\rangle, |ab\rangle, |t\rangle, \theta\}$. We note that to simulate this quantum circuit we used Google's cirq library and opted for the binary counter approach, as it avoids classical controls and keeps our circuit firmly within a quantum setting (The Cirq Developers, 2024). Using our computational model we generated 957,489 sequences contained in 100,000 multi-sequence patterns. We begin by comparing the inter-sequence trends of our generated patterns with Dexter's data. The average depth of each sequence generated has an expected depth of 2.52 compared to Dexter's average sequence lengths of 2.44. Additionally the probability that a protist stays attached after k contractions is roughly $\frac{1}{2^k}$ which is similar to Dexter's experimentally determined probability. In fact, as Dexter et. all observed, the probability that the protist remains attached after n contractions can be fit to an exponential random variable of $0.976e^{-0.6890}$. Note that this parametrization implies that the probability of detachment after any number of contraction is $1 - e^{0.689} \approx 0.498$.

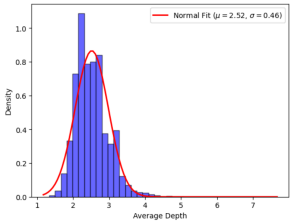

(a) Average depth across 957,489 generated sequences

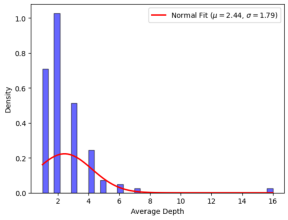

(b) Average depth across 109 experimental sequences

Figure 2: Comparison of average sequence depth between generated and experimental datasets

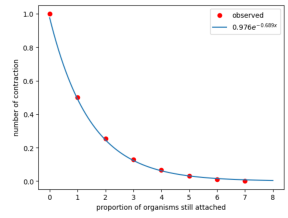

(a) Proportion of protists attached after n contractions across 957,489 generated sequences

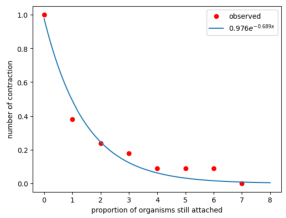

(b) Proportion of protists attached after n contractions across 109 experimental sequences

Figure 3: Comparison of protist attachment dynamics between generated and experimental sequences

Next we compare the intra-sequence trends of our generated patterns with Dexter's data. As expected, we observe that in a multi-sequence pattern, the probability that AB is chosen first converges to 0.30 while the probability that C is chosen first converges to 0.70. While Dexter's dataset only has 56 multi-sequence patterns, we still observe a similar trend. In short, our quantum model is capable of reproducing the statistical trends observed in Dexter's data. Additionally across the 957,489 generated sequences 87 of Dexter's 109 experimentally determined sequences were exactly reproduced.

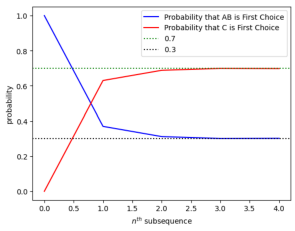

(a) C or AB chosen first in 100,000 generated multi-sequence patterns

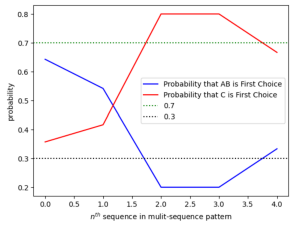

(b) C or AB chosen first in 56 experimental multi-sequence patterns (Dexter et al., 2019)

Figure 4: Comparison of initial action choice (C or AB) in multi-sequence patterns between generated and experimental data

Conclusion

In this paper, we explored the complexity of decision making in the single-celled Stentor roselii. Through an analysis of the data provided by Dexter, we confirmed that the protist's behavioral responses follow statistical trends that imply a form of elementary learning and context-sensitive decision making. The quantum framework we introduced successfully simulates the organism's decision-making process by incorporating both noise and probabilistic features observed in Stentor roselii's behavior. By utilizing quantum statistical theory, particularly quantum circuits with amplitude dampening and memory effects, our model captures the stochastic and history-based nature of the protist's decision-making hierarchy. This allows for the representation of inter- and intra-sequence learning that was absent in earlier models. While the successful application of quantum statistical theory to behavioral decision-making in a single-celled organism does not demonstrate that the organism is in fact using quantum physics in its sensing of environmental information or in its evaluation and implementation of potential responses, the fact that a single-celled organism can engage in a hierarchical decision process opens for the possibility that quantum-scale physical processes are involved in information processing at the cellular level. Since natural selection has had unrestricted access to quantum physics for billions of years, what we need to understand and model is the kind and range of challenges quantum processes can potentially help an organism overcome. The behavior of Stentor roeselii is consistent with the principled prediction that quantum physics may be enabling cellular subsystems to lower metabolic information-processing costs by miniaturizing physical tokens, dampening noise, tracking probabilities, and minimizing heat loss.

References

Asogwa, C. (2019). Quantum biology: Can we explain olfaction using quantum phenomenon? *arXiv preprint arXiv:1911.02529*.

Bohm, D., & Bub, J. (1966). A proposed solution of the measurement problem in quantum mechanics by a hidden variable theory. *Reviews of Modern Physics*, *38*(3), 453.

Bohm, D., & Hiley, B. J. (2006). *The undivided universe: An ontological interpretation of quantum theory*. Routledge.

Bray, D. (2009). *Wetware: a computer in every living cell*. Yale University Press.

De Broglie, L. (1927). La mécanique ondulatoire et la structure atomique de la matière et du rayonnement. *J. Phys. Radium*, *8*(5), 225–241.

Dexter, J. P., Prabakaran, S., & Gunawardena, J. (2019). A complex hierarchy of avoidance behaviors in a single-cell eukaryote. *Current biology*, *29*(24), 4323–4329.

Engel, G. S., Calhoun, T. R., Read, E. L., Ahn, T.-K., Mančal, T., Cheng, Y.-C., ... Fleming, G. R. (2007, April). Evidence for wavelike energy transfer through quantum coherence in photosynthetic systems. *Nature*, *446*(7137), 782–786. Retrieved from http://dx.doi.org/10.1038/nature05678 doi: 10.1038/nature05678

Fields, C., & Levin, M. (2021). Metabolic limits on classical information processing by biological cells. *BioSystems*, *209*, 104513.

Fitch, W. T. (2023). Cellular computation and cognition. *Frontiers in Computational Neuroscience*, *17*, 1107876.

Fleming, G. R., Scholes, G. D., & Cheng, Y.-C. (2011). Quantum effects in biology. *Procedia Chemistry*, *3*(1), 38-57. (22nd Solvay Conference on Chemistry) doi: https://doi.org/10.1016/j.proche.2011.08.011

Gershman, S. J., Balbi, P. E., Gallistel, C. R., & Gunawardena, J. (2021). Reconsidering the evidence for learning in single cells. *Elife*, *10*, e61907.

Giurgica-Tiron, T., Kerenidis, I., Labib, F., Prakash, A., & Zeng, W. (2022, June). Low depth algorithms for quantum amplitude estimation. *Quantum*, *6*, 745. Retrieved from http://dx.doi.org/10.22331/q-2022-06-27-745 doi: 10.22331/q-2022-06-27-745

Hennessey, T. M., Rucker, W. B., & McDiarmid, C. G. (1979). Classical conditioning in paramecia. *Animal learning & behavior*, *7*(4), 417–423.

Jennings, H. S. (1931). 11. introduction and behavior of cœlenterata. In *Behavior of the lower organisms* (pp. 188–232). New York Chichester, West Sussex: Columbia University Press. Retrieved 2024-09-15, from https://doi.org/10.7312/jenn90464-011 doi: doi:10.7312/jenn90464-011

Kundu, S., Dani, R., & Makri, N. (2022). Tight inner ring architecture and quantum motion of nuclei enable efficient energy transfer in bacterial light harvesting. *Science Advances*, *8*(43), eadd0023.

Laughlin, S. B., de Ruyter van Steveninck, R. R., & Anderson, J. C. (1998). The metabolic cost of neural information. *Nature neuroscience*, *1*(1), 36–41.

Lerner, O. (2024). *Boltzmann state-dependent rationality.* arXiv. Retrieved from https://arxiv.org/abs/2404.17725 doi: 10.48550/ARXIV.2404.17725

Marshall, W. F. (2019, December). Cellular cognition: Sequential logic in a giant protist. *Current Biology*, *29*(24), R1303–R1305. Retrieved from http://dx.doi.org/10.1016/j.cub.2019.10.034 doi: 10.1016/j.cub.2019.10.034

Moazed, K. T. (2023). *Quantum biology of the eye: Understanding the essentials*. Springer Nature.

Nielsen, M. A., & Chuang, I. L. (2012). *Quantum Computation and Quantum Information: 10th Anniversary Edition* (10th Anniversary ed.). Cambridge University Press. doi: 10.1017/CBO9780511976667

Oriols, X., & Mompart, J. (2012). *Overview of bohmian mechanics.* arXiv. Retrieved from https://arxiv.org/abs/1206.1084 doi: 10.48550/ARXIV.1206.1084

Picard, M., & Shirihai, O. S. (2022a). Mitochondrial signal transduction. *Cell metabolism*, *34*(11), 1620–1653.

Picard, M., & Shirihai, O. S. (2022b). Mitochondrial signal transduction. *Cell Metabolism*, *34*(11), 1620–1653.

Pothos, E. M., & Busemeyer, J. R. (2013). Can quantum probability provide a new direction for cognitive modeling? *Behavioral and Brain Sciences*, *36*(3), 255–274. doi: 10.1017/s0140525x12001525

Pyke, G. (2019). Optimal foraging theory: an introduction. In *Encyclopedia of animal behavior* (p. 111-117). Elsevier Academic Press.

Quian Quiroga, R., Boscaglia, M., Jonas, J., Rey, H. G., Yan, X., Maillard, L., ... Rossion, B. (2023, September). Single neuron responses underlying face recognition in the human midfusiform face-selective cortex. *Nature Communications*, *14*(1). Retrieved from http://dx.doi.org/10.1038/s41467-023-41323-5 doi: 10.1038/s41467-023-41323-5

Savelli, F., & Knierim, J. J. (2018). *Ai mimics brain codes for navigation.* Nature Publishing Group UK London.

Serrano, S., Arregui, L., Perez-Uz, B., Calvo, P., & Guinea, A. (2015, December). Guidelines for the identification of ciliates in wastewater treatment plants. *Water Intelligence Online*, *7*(0), 9781780401935–9781780401935. Retrieved from http://dx.doi.org/10.2166/9781780401935 doi: 10.2166/9781780401935

Shirakawa, T., Gunji, Y.-P., & Miyake, Y. (2011). An associative learning experiment using the plasmodium of physarum polycephalum. *Nano communication networks*, *2*(2-3), 99–105.

Staddon, J. E. R. (2016). *Adaptive behavior and learning*. Cambridge University Press.

Tartar, V. (2013). *The biology of stentor: International se-*

ries of monographs on pure and applied biology: Zoology. Elsevier.

The Cirq Developers. (2024). *Cirq: A python framework for creating, editing, and invoking noisy intermediate scale quantum (nisq) circuits.* https://quantumai.google/cirq. Retrieved from https://github.com/quantumlib/Cirq (Accessed: 2024-05-10)

Trinh, M. K., Wayland, M. T., & Prabakaran, S. (2019, December). Behavioural analysis of single-cell aneural ciliate, stentor roeseli, using machine learning approaches. *Journal of The Royal Society Interface*, *16*(161), 20190410. Retrieved from http://dx.doi.org/10.1098/rsif.2019.0410 doi: 10.1098/rsif.2019.0410

Uthailiang, T., Suntijitrungruang, O., Issarakul, P., Pongkitiwanichakul, P., & Boonchui, S. (2025). Investigation of quantum trajectories in photosynthetic light harvesting through a quantum stochastic approach. *Scientific Reports*, *15*(1), 5220.

Wang, B.-X., Tao, M.-J., Ai, Q., Xin, T., Lambert, N., Ruan, D., ... Long, G.-L. (2018). Efficient quantum simulation of photosynthetic light harvesting. *NPJ Quantum Information*, *4*(1), 52.

Wang, Z., Busemeyer, J. R., Atmanspacher, H., & Pothos, E. M. (2013). The potential of using quantum theory to build models of cognition. *Topics in Cognitive Science*, *5*(4), 672–688. doi: 10.1111/tops.12043

Wigner, E. P. (1963). The problem of measurement. *American Journal of Physics*, *31*(1), 6–15.

Wood, D. C. (1969). Parametric studies of the response decrement produced by mechanical stimuli in the protozoan, stentor coeruleus. *Journal of neurobiology*, *1*(3), 345–360.

Xie, C. (2022). Searching for unity in diversity of animal magnetoreception: From biology to quantum mechanics and back. *The Innovation*, *3*(3).

Yukalov, V. I., & Sornette, D. (2014). Conditions for quantum interference in cognitive sciences. *Topics in Cognitive Science*, *6*(1), 79–90. doi: 10.1111/tops.12065